Journal of the American College of Cardiology
© 2001 by the American College of Cardiology
Published by Elsevier Science Inc.

Vol. 37, No. 6, 2001
ISSN 0735-1097/01/$20.00
PII S0735-1097(01)01192-5

Multiple Atrial Macro–Re-entry Circuits in Adults With Repaired Congenital Heart Disease: Entrainment Mapping Combined With Three-Dimensional Electroanatomic Mapping

Etienne Delacretaz, MD,* Leonard I. Ganz, MD, FACC,* Kyoko Soejima, MD,* Peter L. Friedman, MD, PHD, FACC,* Edward P. Walsh, MD, FACC,* John K. Triedman, MD, FACC,* Laurence J. Sloss, MD, FACC,† Michael J. Landzberg, MD, FACC,† William G. Stevenson, MD, FACC*

Boston, Massachusetts

OBJECTIVES We sought to characterize re-entry circuits causing intra-atrial re-entrant tachycardias (IARTs) late after the repair of congenital heart disease (CHD) and to define an approach for mapping and ablation, combining anatomy, activation sequence data and entrainment mapping.

BACKGROUND The development of IARTs after repair of CHD is difficult to manage and ablate due to complex anatomy, variable re-entry circuit locations and the frequent co-existence of multiple circuits.

METHODS Forty-seven re-entry circuits were mapped in 20 patients with recurrent IARTs refractory to medical therapy. In the first group (n = 7), ablation was guided by entrainment mapping. In the second group (n = 13), entrainment mapping was combined with a three-dimensional electroanatomic mapping system to precisely localize the scar-related boundaries of re-entry circuits and to reconstruct the activation pattern.

RESULTS Three types of right atrial macro–re-entrant circuits were identified: those related to a lateral right atriotomy scar (19 IARTs), the Eustachian isthmus (18 IARTs) or an atrial septal patch (8 IARTs). Two IARTs originated in the left atrium. Radiofrequency (RF) lesions were applied to transect critical isthmuses in the right atrium. In three patients, the combined mapping approach identified a narrow isthmuses in the lateral atrium, where the first RF lesion interrupted the circuit; the remaining circuits were interrupted by a series of RF lesions across a broader path. Overall, 38 (81%) of 47 IARTs were successfully ablated. During follow-up ranging from 3 to 46 months, 16 (80%) of 20 patients remained free of recurrence. Success was similar in the first 7 (group 1) and last 13 patients (group 2), but fluoroscopy time decreased from 60 ± 30 to 24 ± 9 min/procedure, probably related to the increasing experience and ability to monitor catheter position non-fluoroscopically.

CONCLUSIONS Entrainment mapping combined with three-dimensional electroanatomic mapping allows delineation of complex re-entry circuits and critical isthmuses as targets for ablation. Radiofrequency catheter ablation is a reasonable option for treatment of IARTs related to repair of CHD. (J Am Coll Cardiol 2001;37:1665–76) © 2001 by the American College of Cardiology

Intra-atrial re-entrant tachycardias (IARTs) are common late after surgical repair of congenital heart disease (CHD) and frequently cause troublesome symptoms and hemodynamic compromise. Medical therapy is accompanied by potential side effects, including bradyarrhythmias and life-threatening pro-arrhythmia, and is often ineffective. Catheter ablation has been remarkably successful for the management of patients with common atrial flutter dependent on conduction of the circulating wave front through an isthmus created by the tricuspid valve annulus and inferior vena cava (1). Although patients with repaired CHD can have counterclockwise or clockwise isthmus-dependent atrial flutter, other re-entry circuits related to atrial incisions and patches also occur (2). These circuits can be difficult to identify and interrupt. Conventional activation mapping is difficult because of the complicated re-entry paths, multiple potential re-entry loops and presence of fractionated and low-amplitude electrograms. Entrainment mapping can be used to determine which sites are in a re-entry circuit and to guide radiofrequency (RF) ablation (2,3). However, it is often difficult to identify a narrow isthmus with entrainment mapping alone (4). Furthermore, the complex atrial anatomy after surgery makes it difficult to fluoroscopically identify the exact catheter position, in relation to anatomic structures and regions of scars. A three-dimensional electroanatomic mapping system has recently become available, allowing the endomyocardial activation sequence data and electrogram voltage to be superimposed on the geometry of the heart cavities (5–7). Association of this new technique with entrainment mapping has been proposed to define scar-related macro–re-entrant circuits.

From the *Cardiac Arrhythmia Service and Clinical Electrophysiology Laboratory, Children's Hospital; and †Boston Adult Congenital Service, Brigham and Women's Hospital, Harvard Medical School, Boston, Massachusetts. Dr. Delacretaz was supported by a grant from the Swiss Society of Cardiology (Cardiac Pacing and Electrophysiology Working Group).

Manuscript received October 8, 1999; revised manuscript received December 28, 2000, accepted January 18, 2001.

JACC Vol. 37, No. 6, 2001
May 2001:1665–76

Abbreviations and Acronyms

ASD = atrial septal defect
CHD = congenital heart disease
ECG = electrocardiogram or electrocardiographic
IART = intra-atrial re-entrant tachycardias
PPI = post-pacing interval
RF = radiofrequency
TCL = tachycardia cycle length

The aims of this study were: 1) to describe entrainment and electroanatomic mapping characterization of the different circuits encountered in IARTs; 2) to evaluate the effect of RF ablation; 3) to compare ablation guided by entrainment alone versus entrainment combined with electroanatomic mapping; and 4) and to assess the relation between the post-pacing interval (PPI) during entrainment mapping and re-entry circuit sites in IART. Accordingly, ablation was guided by entrainment in the first 7 patients (group 1) and by a combined approach in the next 13 patients (group 2).

METHODS

The patient group consisted of 20 patients with a history of remote surgical repair of CHD, who were referred for electrophysiologic study and RF catheter ablation of IARTs refractory to anti-arrhythmic drug therapy (Table 1).

Electrophysiologic study. All studies were performed after the subjects provided written, informed consent according to institutional guidelines consistent with the policies of the institutional Committee on Human Research. Quadripolar electrode catheters were placed in the high right atrium, His bundle position and right ventricular apex through the femoral veins. Decapolar catheters were positioned in the coronary sinus or right atrium, or both. Right atrial mapping was performed with a 7F catheter with a 4-mm tip electrode (EP Technologies, Sunnyvale, California; or Cordis-Webster, Sunnyvale, California). Conscious sedation was achieved with intermittent doses of midazolam and fentanyl. After catheter placement, the patients received an intravenous bolus of heparin (5,000 U) and then 1,000 U hourly. Surface electrocardiographic (ECG) and intracardiac bipolar signals were filtered at 30 to 500 Hz and recorded on a digital acquisition system (Cardiolab, Prucka Engineering, Inc., Houston, Texas).

During mapping, potential obstacles to conduction (atriotomy scar, atrial septal defect [ASD] patch) were identified, during sinus rhythm and IART. Regions with very low signal amplitude, double potentials and striking changes in signal amplitude and/or timing, with very small changes in catheter position, and failure to capture during unipolar pacing at 10 mA, 2 ms pulse width, despite apparently good electrode tissue contact, were believed to signify anatomic barriers to conduction.

Entrainment mapping. Entrainment mapping was attempted for all sustained IARTs at various sites in the right atrium, initially focusing on the Eustachian isthmus at sites close to the areas of scar detected (4). A train of 8 to 12 unipolar stimuli was delivered from the distal electrode of the mapping catheter at a cycle length 10 to 40 ms shorter than the tachycardia cycle length (TCL). Pacing at 2 ms and 10 mA was used for entrainment. Stimulus strength was increased to 5- and 9-ms pulse width when the initial train failed to capture the atrium. Analysis of entrainment at a site required acceleration of all electrograms to the pacing rate, a stable sequence of activation after the first few stimuli and return of the same atrial tachycardia activation sequence on the first beat after pacing. If the tachycardia was entrained, the PPI was measured from the last stimulus artifact to the return electrogram that occurred at an interval closest to the TCL, provided that the electrogram did not appear to be a "far-field electrogram" during pacing (see subsequent text). This pacing site electrogram was usually recorded either from the most distal bipole (electrodes 1 and 2) or, when this was obscured by the stimulus artifact, from a more proximal bipole (electrodes 2 and 3). In regions with double potential or multiple potentials, we entrained tachycardia and evaluated which potentials were captured by the pacing stimulus (Fig. 1). Electrogram potentials that were present before each stimulus, such that they could not be directly captured by the stimulus, were defined as "far-field" potentials. Sites at which the PPI closely approximated the TCL ($\leq$30 ms difference) were classified as those within the re-entry circuit (Fig. 2). No attempt was made during the procedure to assess whether entrainment occurred with manifest or concealed fusion (without a significant change in surface p wave morphology or atrial activation sequence). Fusion was assessed retrospectively, however, by comparison of the surface p wave morphology (Fig. 2).

Electroanatomic mapping. In the last 13 patients, mapping was performed by using an electromagnetic catheter location system (CARTO, Biosense-Cordis-Webster, Inc., Baldwyn Park, California). A three-dimensional activation sequence map of the right atrium during IART was constructed during 18 of 23 tachycardias in these 13 patients (Fig. 2, 3 and 4) (7). Anatomic and electrophysiologic landmarks (those of the inferior and superior vena cava, coronary sinus, His bundle and tricuspid annulus) were marked. Entrainment mapping of IARTs at candidate sites possibly critical to the IART circuit (close to the lateral right atrial scar, inter-atrial septum and right atrial inferior isthmus) was performed to determine whether these sites were in the macro–re-entrant circuit or were bystander potentials. Detailed activation mapping of areas with short PPI–TCL differences was performed (Fig. 2, 3 and 4). When two potentials were present, the CARTO system was configured to initially select the potential with the fastest negative slope as the site of activation. At selected double-potential sites, we entrained tachycardia and evaluated which potentials were captured by the pacing stimulus (Fig. 1). Local activation times were reviewed, and the apparent

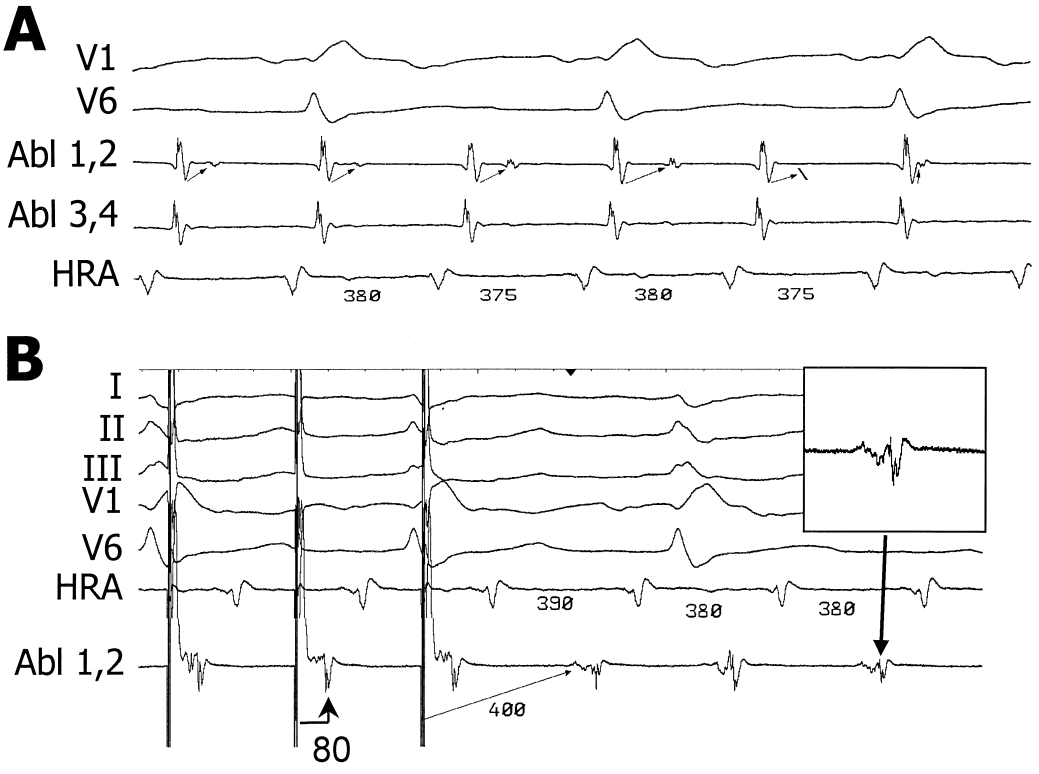

Figure 1. Tracings show examples of fractionated electrograms and bystander and far-field potentials. Shown, from top to bottom, are surface ECG leads I, III, V_1 and V_6, filtered bipolar recordings from the distal (ablation [Abl] 1 and 2) and proximal (Abl 3 and 4) electrode pair of the mapping catheter and intra-cardiac recordings from the high right atrium (HRA). **(A)** Atrial tachycardia with a cycle length of 380 ms. The ablation catheter positioned at the lateral atriotomy scar records a double potential with intra-atrial Wenckebach conduction to the second potential, exposing that signal as a bystander potential that is not critical to the tachycardia, which continues regardless of the timing of the far-field potential. **(B)** Entrainment of the atrial tachycardia from a site in the lateral right atrium. During tachycardia (last 3 atrial beats), there was a fractionated signal lasting 90 ms (shown at greater magnification in the **inset**, corresponding to the **arrow** at the last beat); therefore, precise timing of the local activation is difficult. The last three stimuli of a pacing train at 340 ms are shown; during unipolar pacing, the second component of the signal with the largest rapid deflection is entrained with a delay of 80 ms, suggesting that this component of the electrogram is a far-field signal, and the first, lower voltage component of the signal corresponds to the myocardium that is directly captured by the pacing stimulus, and therefore to local activation. After cessation of pacing, the PPI, measured to the low-amplitude deflection of the signal recorded by the ablation catheter, is 400 ms, 20 ms longer than the TCL, consistent with a close proximity to the re-entry circuit. Failure to recognize the actual local electrogram and measurement of the PPI to the largest deflection would lead to misclassification of this site as "out of the circuit," with a PPI of 470 ms, 90 ms longer than the TCL.

"far-field" signal was excluded from the activation maps. A map displaying the bipolar electrogram's maximal voltage was generated and used to identify areas of low-amplitude electrogram consistent with scar. A color-coded local activation time map (Fig. 2, 3 and 4) and animated propagation (Fig. 2D and 3B) were analyzed to determine the activation pattern, particularly in relation to conduction barriers.

Catheter ablation. Ablation sites were selected as follows: 1) the site was in the circuit by entrainment mapping; 2) the site was between two unexcitable regions (scar, valve annulus or great vessel), creating an isthmus that could be transected; and 3) for sites in the lateral right atrium, phrenic nerve stimulation was absent during unipolar pacing at 10 mA, 2 ms stimulus strength. Power (maximum 50 W) was titrated to achieve a temperature of 60°C or a fall in impedance of 5 to 10 ohm. If the Eustachian isthmus was in the circuit, this region was transected with ablation lesions. If the lateral right atrial wall, but not the Eustachian isthmus, was in the circuit, detailed mapping of the lateral right atrium was performed, looking for a narrow isthmus between regions of scar. If a narrow isthmus was not identified, a line of lesions was placed between an area of right atrial scar and another anatomic barrier (vena cava or tricuspid annulus) to transect the circuit, after entrainment indicated that those regions along the intended line were in the re-entry circuit. If tachycardia terminated during RF application, the line of RF lesions was completed. If attempted entrainment changed the tachycardia circuit, activation mapping was performed with minimal attempts to entrain the tachycardia. If only the septum was in the circuit, a similar approach was taken, defining a line to interrupt the circuit between the septal patch and the superior or inferior vena cava, or another obstacle to conduction.

The end point of ablation was tachycardia termination and completion of the series of RF lesions across the critical isthmus. For ablation across the Eustachian isthmus, bidirectional conduction block was assessed during pacing from the coronary sinus and low lateral right atrium. However, conduction block across the line of lesions was not assessed systematically in the other types of circuits.

After ablation, attempts were made to re-induce tachy-

Table 1. Clinical and Electrophysiological Characteristics *(continued on next page)*

Pt. No.	Congenital Defect	Surgical Repair	Drugs That Failed	Circuit Isthmus Location	Atrial TCL (ms)	PPI–TCL at Termination Site
1*	ASD	ASD repair	Ca, D, B	Septal	360	0
				Eustachian	490	5
				Lat. RA	325	0
				Lat. RA	300	0
				Septal	260	0
2*	ASD, PPS, Eisenmenger's	ASD repair	Ca, B, D	Septal	275, 315	0, 35
				Septal	285	0
3	TOF	Complete repair	Proc, Q, PPF, D, Diso	Lat. RA	280	20
				Eustachian (2)	215, 215	0
4*	TGV, VSD, PS	LV-PA conduit, VSD repair	D, Ca, Q, S	Eustachian (2)	315, 315	25
				Lat. RA	315	0
5	ASD, anomalous PVR	ASD repair	D, B, S	Lat. RA	280–290	5
				Eustachian	300	
				Septal	340	
6	ASD (HOLT-ORAM)	ASD repair	D, Ca, B, Diso, F	Lat. RA	245	NA
7	TOF	Complete repair	D, Q, PPF, S, B, Amio	Lat. RA	525	0
				Eustachian	380	5
				Left atrium	460–425	NA
8‡	ASD	ASD repair	B, Q	Eustachian	210–190	0
				Lat. RA (2)	210–190	25
9‡	TOF	Complete repair	D	Eustachian	360	NA
				Lat. RA	270	NA
				Septal	250–300	NA
10‡	Ebstein's, ASD	TV repair, ASD repair	D, Q	Eustachia (2)	295, 270	NA
				Lat. RA (2)	230, 300	NA
				Septal	235	NA
11‡	TOF	Complete repair	D, B	Lat. RA (3)	500, 495, 260	NA
12‡	PDA, VSD	PDA ligation, VSD and ASD repairs	D, Ca	Eustachian	310	0
				Lat. RA	300	0
13‡	DORV, VSD, ASD	VSD and AVR repairs, Konno procedure	B, D, S	Lat. RA	320	0
14‡	TOF	Complete repair	Q, Amio, D	Eustachian	370	0
15‡	ASD	ASD repair	D, Proc, Amio, Diso	Eustachian	400	0
16‡	TGV, VSD	Mustard procedure, VSD repair	Q, Proc	Lat. RA	250	0
				Left atrium	290	NA
17‡	ASD	ASD repair	Q	Eustachian	340	0
18‡	ASD	ASD repair	Q, D, B	Eustachian	240	0
				Lat. RA	260	0
19‡	ASD	ASD repair		Eustachian	270	0
20‡	ASD	ASD repair	None	Eustachian	310	0

Numbers in parentheses indicate the number of tachycardia circuits with that finding. * Patients had repeat procedures because of one early (<3 months, Patient nos. 1 and 2) and one late recurrence (Patient nos. 2 and 4) of tachyarrhythmia. †Ablation was diverted because pacing at the intended ablation sites stimulated the phrenic nerve. ‡Patients who underwent entrainment mapping combined with electroanatomic mapping.

AAD = anti-arrhythmic drug; Amio = amiodarone; ASD = atrial septal defect; AVR = aortic valve replacement; B = beta-blocker; Ca = calcium channel blocker; CS = coronary sinus; D = digoxin; Diso = disopyramide; DORV = double-outlet right ventricle; F = flecainide; F/U = follow-up; HOLT-ORAM = Holt-Oram Syndrome; IVC = inferior vena cava; Lat. = lateral; LV-PA = left ventricle to pulmonary artery; NA = not available; n.s. = not successful; no RF = radiofrequency ablation was not attempted; PAF = paroxysmal atrial fibrillation; PDA = patent ductus arteriosus; PPF = propafenone; PPI = post-pacing interval; PPS = peripheral pulmonic stenosis; Proc = procainamide; PS = pulmonic stenosis; PVR = pulmonary venous return; Q = quinidine; RA = right atrium; RF = radiofrequency; S = sotalol; s. = successful; SVC = superior vena cava; TA = tricuspid annulus; TCL = tachycardia cycle length; TGV = L-transposition of great vessels; TOF = tetralogy of Fallot; TV = tricuspid valve; VSD = ventricular septal defect.

cardia, using two to three atrial extrastimuli at two paced cycle lengths, as well as burst atrial pacing. Ablation was considered successful if no sustained monomorphic IART was inducible after the ablation procedure. Long-term success was defined as the absence of any spontaneous sustained IART during follow-up.

Follow-up. After ablation, patients were monitored for symptomatic recurrences and ECGs were obtained in the clinic; routine, long-term ambulatory recordings were not used. Anti-arrhythmic drug therapy was continued in patients with a history of atrial fibrillation or when RF ablation did not abolish all inducible tachycardias.

Continuous variables are expressed as the mean value ± SD and are compared using the two-tailed unpaired *t* test. Cumulative risk of recurrence was calculated using the Kaplan-Meier method.

Table 1. *(continued from previous page)*

Design of Ablation Line Created	No. RF Lesions	Acute RF Effect	F/U AAD Therapy	Clinical Recurrence	F/U Month
High anteroseptal to posteroseptal	20	s.	None	Yes	(30)
CS-TA		s.			
Lat. RA-IVC	15	s.	None	Yes	(29)
Lat. RA-TA	15	s.	S	No	17
FO-TA		n.s.			
FO-SVC	13	s. (2)	None	Yes	(42)
FO-SVC	40	s.	None	No	38
Lat. RA-IVC	23	s.	None	No	24
IVC-TA		s. (2)			
IVC-TA	19	s. (2)	D	Yes	(37)
Lat. RA-TA	14	s.	D	No	9
Lat. RA-TA	106	s.	B	No	36
TA-IVC		s.			
FO-IVC		s.			
IVC–anterolateral RA–SVC	37	n.s.	D	Yes	46
Anterolateral RA-TA					
TA-IVC					
Lat. RA-TA	24	s.	S	No	45
IVC-TA		s.			
Not attempted		no RF			
IVC-TA	35	s.	Amio	PAF after 17 months	35
Lat. RA-TA		s. (2)			
IVC-TA	24	s.	B, D	No	15
Lat. RA-TA		s.			
FO-IVC-CS		s.			
IVC-TA, CS-TA	91	s. (2)	D, Q	No	25
Lat. RA-TA		s. (2)			
FO-TA		n.s.			
SVC-IVC lat. RA	18	n.s. (3)†	Amio	Yes	16
IVC-TA	15	s.	D, Ca	Yes	13
Lat. RA-IVC		n.s.†			
Lat. RA–Lat. RA	6	s.	D	No	14
IVC-TA	6	s.	D, Amio	No	7
IVC-TA	11	s.	D	No	7
Lat. RA-IVC, Lat. RA–TA, mitral annulus-post scar	45	s. n.s.	None	No	7
IVC-TA	4	s.	None	Yes	4
IVC-TA	51	s.	None	No	6
Lat. RA–Lat. RA		s.			
IVC-TA	21	s.	None	No	6
IVC-TA	2	s.	None	No	3

RESULTS

The clinical characteristics of the 20 patients are outlined in Table 1. The patients' mean age was 43 ± 15 years (range 29 to 72). Patients had experienced symptoms refractory to a mean of 1.8 (median 2) anti-arrhythmic drugs and a mean of 1.1 (median 1) atrioventricular node-blocking agents before the study. A total of 47 IARTs were induced in these 20 patients (2.4 tachycardias/patient; Table 1). Forty-five of the 47 tachycardias originated in the right atrium, and 2 tachycardias originated in the left atrium.

Characteristics of three types macro–re-entrant circuits. Three general types of right atrial macro–re-entrant circuits were identified: those related to the lateral atriotomy scar; typical clockwise or counterclockwise atrial flutter circuits utilizing the isthmus between the tricuspid annulus and the inferior vena cava; and re-entry around an ASD patch.

MACRO–RE-ENTRY INVOLVING THE LATERAL ATRIOTOMY SCAR. Re-entry related to the lateral atriotomy scar was inducible in 15 of 20 patients and was the most common circuit found in the study group (19 IARTs) (Fig. 2 and 3). With entrainment mapping, the PPI–TCL difference was <30 ms when pacing at the superior and inferior margins of the right atrial atriotomy scar, but longer when pacing from the right atrial inferior isthmus, between the tricuspid annulus and inferior vena cava, and from the inter-atrial septum. In three patients, electro-anatomic mapping combined with entrainment led to identification of a narrow isthmus between two areas of

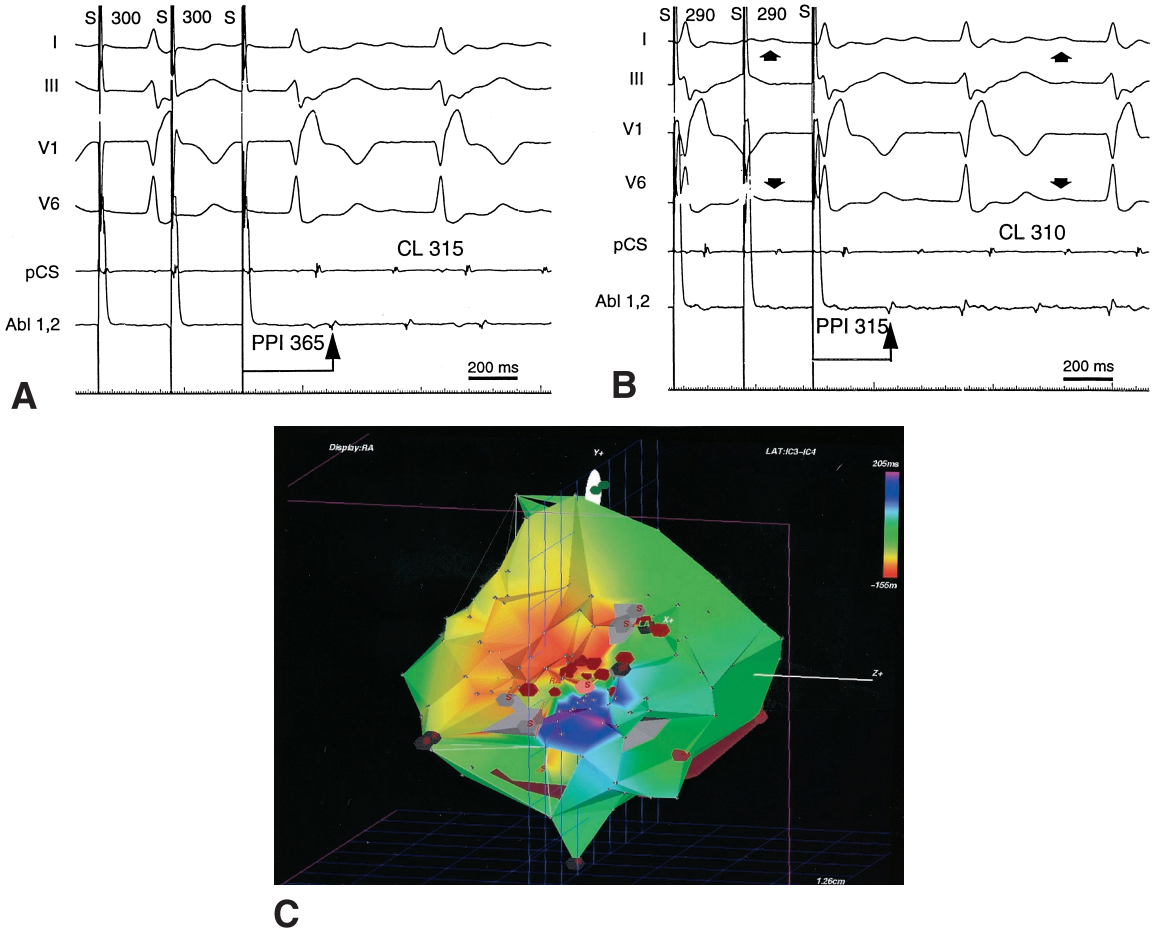

Figure 2. Entrainment of IARTs by pacing from two different sites in a patient with previous repair of atrial and ventricular septal defects, as well as aortic valve replacement for a double-outlet right ventricle. Shown, from top to bottom, are surface ECG leads I, III, V_1 and V_6, intra-cardiac recordings from the proximal coronary sinus (pCS) and filtered bipolar recordings (ablation [Abl] 1 and 2) from the mapping catheter. **(A)** Pacing is performed at a site remote from the tachycardia circuit, at the lateral entrance of the infero-lateral right atrium (**brown tag** at low anterior right atrium in **panel C**). The tachycardia cycle length (CL) is 315 ms. The last three stimuli (S) of a pacing train at 300 ms are shown; pacing accelerates the tachycardia to the pacing rate (entrainment). After cessation of pacing, the PPI, measured to the local bipolar electrogram recorded from the distal pair of electrodes in the ablation catheter, is 365 ms, 50 ms longer than the TCL, indicating that the site is outside of the re-entry circuit. Long PPIs during entrainment from the mid and septal aspects of the Eustachian isthmus confirmed that this tachycardia was not isthmus-dependent (not shown). **(B)** Pacing is performed at the mid lateral right atrium (**pink tag** in **panel C**). The TCL is 310 ms. A pacing train at 290 ms entrains the tachycardia, with a PPI of 315 ms, consistent with a re-entry circuit site. P wave morphology **(downward arrows)** during entrainment appears identical to p wave morphology during tachycardia (entrainment with concealed fusion). **(C–E)** Three-dimensional electroanatomic maps of the same tachycardia as in A and B. **(C)** Activation sequence map of the right atrium (right anterior oblique view) constructed from 165 points acquired during tachycardia. **Gray areas** in the lateral atrium represent unexcitable scar related to previous atriotomy, characterized by very low voltage electrograms. The tricuspid annulus is shown by a **brown circle**. The activation time is color-coded: the **red areas** denote sites of early activation, and **purple** denotes the latest activation. The time scale for color coding is indicated in the bar at the upper right. During tachycardia, the depolarization wave travels from the mid lateral right atrium superiorly. The superior (clockwise) wave front returns to the region proximal to the exit site **(purple)** to complete the circuit by propagating through a narrow isthmus bounded by two areas of unexcitable scar. The pacing site shown in B (in the circuit) was at the **pink tag** in the isthmus between the two scars. The bystander pacing site shown in A was adjacent to the tricuspid annulus (the most rightward and inferiorly located **brown tag**). A series of RF lesions, indicated by the **red tags** extending between two of the gray scar regions, transected this isthmus. Tachycardia terminated during the third lesion **(pink dot)**. The line transecting the isthmus was then completed with additional lesions. (*Figure 2 continued on next page.*)

scar within the lateral right atrium, where a single RF lesion or catheter pressure terminated tachycardia (Fig. 2C and 3A). Thirteen of the remaining tachycardias were abolished by transecting a broader isthmus with a series of lesions. Successful ablation lines extended from the inferior border of the atriotomy scar to the inferior vena cava (3 tachycardias), to the tricuspid annulus (8 tachycardias) and to both the inferior vena cava and tricuspid annulus (1 tachycardia) (Table 1). A line of lesions from the inferior vena cava to the superior vena cava was designed but was not completed in two patients (4 tachycardias), because pacing at sites along the line caused phrenic nerve stimulation, indicating its close proximity. For one patient (1 tachycardia), a complex design of lines of RF was intended, including lines from the inferior vena cava to the superior vena cava, from lateral atrium to the tricuspid annulus and from the inferior vena cava to the tricuspid annulus. Overall, RF ablation successfully abolished 16 of 20 IARTs in 12 of 15 patients.

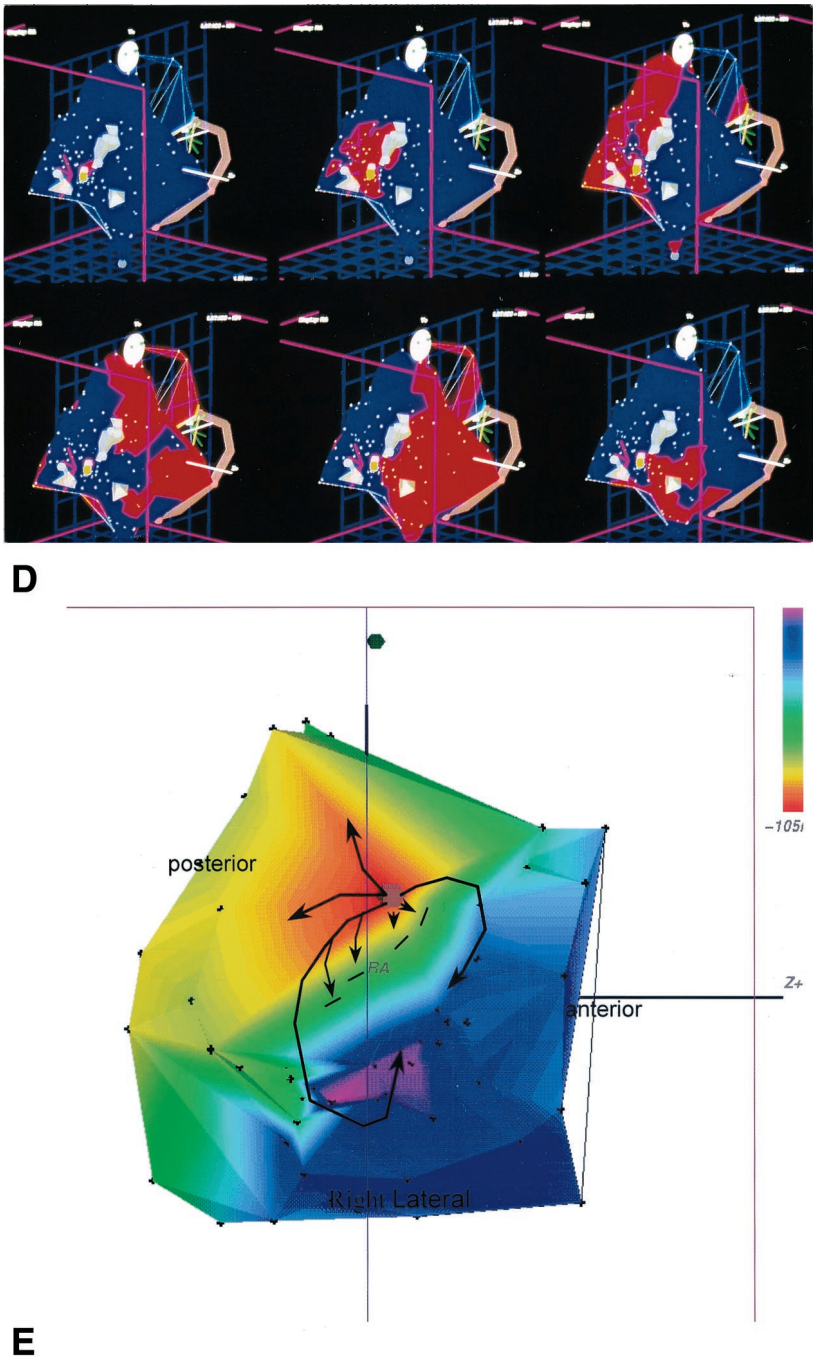

Figure 2. (*Continued from previous page*) **(D)** Propagation map of atrial tachycardia demonstrating a depolarization wave front **(red)** in a right anterior oblique cranial view. As in part A, the **gray zones** outline areas of unexcitable scar; the tricuspid annulus is represented in **brown**; and **brown and pink dots** represent sites where the PPI equaled TCL and where RF ablation successfully terminated tachycardia, respectively. The six frames (from right to left across the top row, followed by right to left in the bottom row) represent the temporal propagation of activation throughout the macro–re-entrant circuit cycle. Areas in **red** represent depolarization within a 30-ms time frame. From the exit of this narrow pathway, a broad proportion of the postero-superior right atrium depolarizes very quickly. The re-entry waves then circle superiorly in the clockwise direction, and inferiorly, colliding with the inferior aspect of the scar. **(E)** After ablation conduction block across the isthmus was demonstrated by pacing from the postero-superior aspect of the line of lesion. Activation procedes around the scar **(arrows)**, arriving at the site opposite the pacing site after 310 ms.

EUSTACHIAN ISTHMUS-DEPENDENT ATRIAL FLUTTER. Eustachian isthmus-dependent atrial flutter was inducible in 13 of 20 patients (18 IARTs). During entrainment, the PPI–TCL difference was <30 ms when pacing from the lateral, mid and septal portions of the right atrial inferior isthmus. In nine patients, counterclockwise atrial flutter was inducible, and in four patients, both clockwise and counterclockwise isthmus-dependent atrial flutter was inducible (Fig. 4B). A series of RF ablation lesions from the tricuspid annulus to the inferior vena cava (n = 12) or coronary sinus (n = 1) successfully abolished all of these IARTs in all 13 patients.

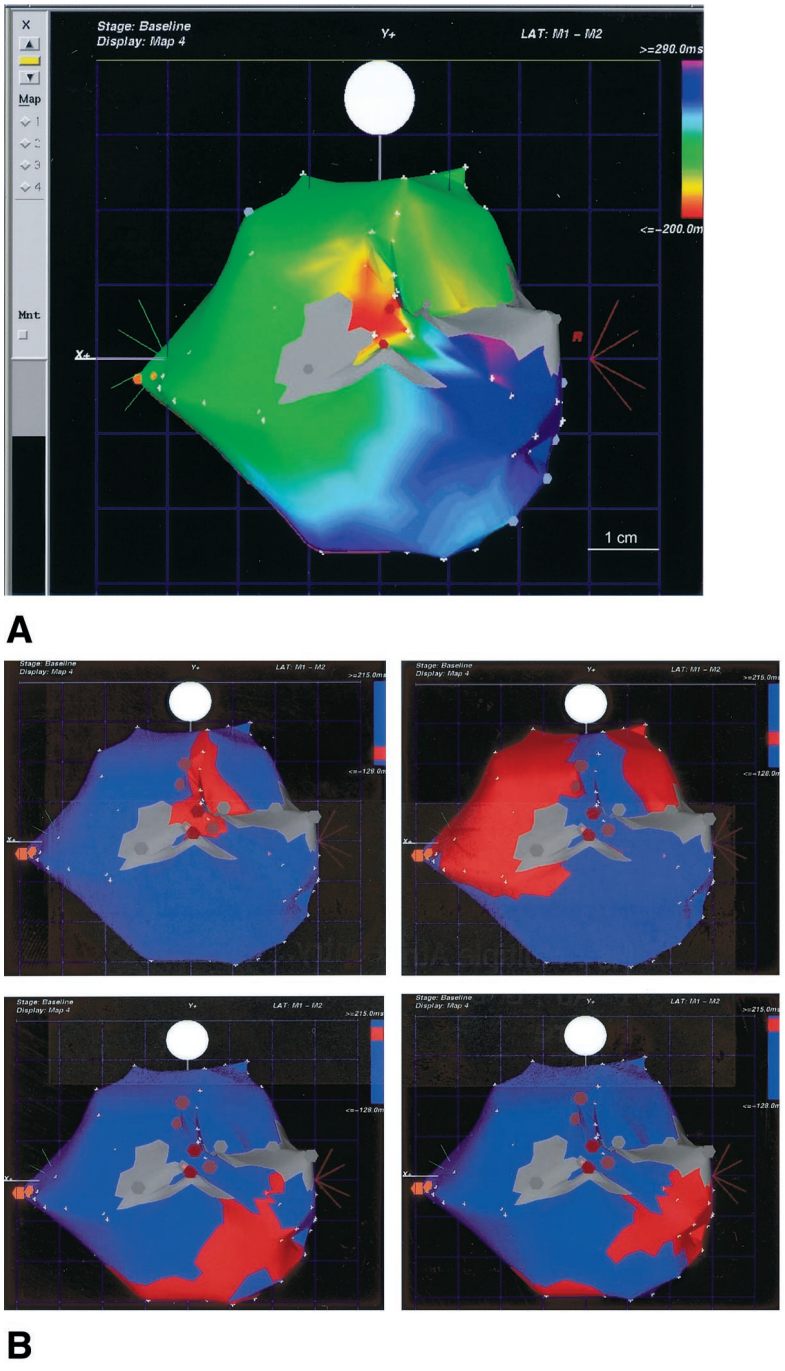

Figure 3. Three-dimensional electroanatomic maps and entrainment mapping of IART in a patient with previous ASD repair. **(A)** Activation sequence map of the right atrium (posterior view) constructed during IART. **Gray areas** in the postero-lateral atrium represent areas of unexcitable scar related to previous atriotomy, characterized by very low voltage electrograms. The **red areas** represents sites of early activation, and **purple** signifies the latest activation. During tachycardia, the depolarization wave travels from the mid posterior right atrium superiorly. A counterclockwise wave front returns to the region proximal to the exit site **(purple)** to complete the circuit by propagating through a narrow isthmus bounded by two areas of unexcitable scar. Tachycardia terminated during the first RF application **(red tag)**. An additional radiofrequency ablation lesion was applied adjacent to the first lesion where pacing captured. Subsequently, no tachycardia was inducible. **(B)** Propagation map of atrial tachycardia demonstrating depolarization wave front **(red)** in a posterior view. As in part A, **gray zones** outline areas of unexcitable scar; **red tags** represent ablation sites; and **brown tags** represent sites where the PPI equaled TCL. The four frames represent the temporal propagation of activation throughout the macro–re-entrant circuit cycle. Areas in **red** represent depolarization within a 40-ms time frame.

RE-ENTRY AROUND AN ASD PATCH. Re-entry involving an ASD patch was demonstrated in 5 of 16 patients (8 IARTs). In four of five patients, this type of tachycardia was recognized during or after RF ablation of the Eustachian isthmus. Long PPIs when pacing from the mid portion of the isthmus after ablation indicated that the circuit had changed. Short PPI–TCL differences were then observed when entraining tachycardia from sites surrounding the

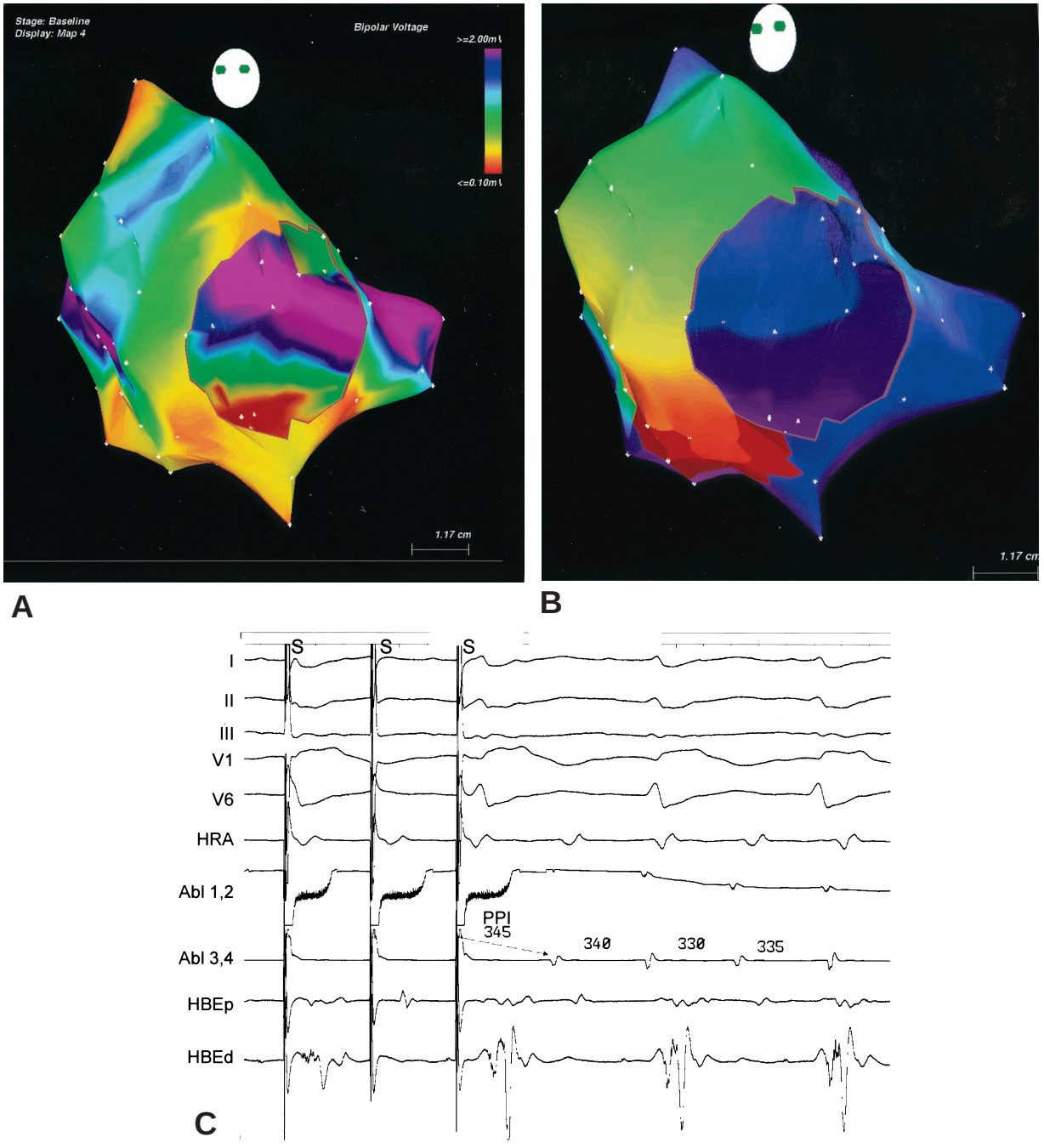

Figure 4. Three-dimensional electroanatomic maps and entrainment mapping from a patient with IART due to clockwise re-entry around the tricuspid annulus late after ASD repair. **(A)** Three-dimensional view of the right atrium, displaying the bipolar electrogram's maximal voltage with color coding, is shown in the left anterior oblique view. The tricuspid annulus is delineated with a **brown line**. The voltage map of the right atrium was constructed by sequential sampling incorporating electrogram-derived bipolar amplitude, as well as spatial coordinates from each of the sites recorded. Areas where the voltage of the electrogram was <0.3 mV are in **red**. Areas where the amplitude of the electrogram was >3.0 mV are in **purple**. An area of scar is delineated on the postero-inferior right atrium, as well as in the high lateral right atrium. **(B)** Activation sequence map of the right atrium in the same left anterior oblique view constructed during IART with a cycle length of 345 ms. During tachycardia, the depolarization wave travels clockwise around the tricuspid annulus. **(C)** Entrainment of tachycardia by pacing from the Eustachian isthmus. Shown, from top to bottom, are surface ECG leads I, II, III, V_1 and V_6, intra-cardiac recordings from the high right atrium (HRA) and filtered bipolar recordings from the distal (ablation [Abl] 1 and 2) and proximal (Abl 3 and 4) electrode pairs of the mapping catheter and proximal and distal His bundle (HBEp and HBEd). The TCL is slightly oscillating at ~335 ms. The last three stimuli (S) of a pacing train at 315 ms are shown. Tachycardia was entrained with a PPI of 345 ms, consistent with a re-entry circuit site.

septal patch. It was not possible to define an entire re-entry circuit in these cases, possibly because a portion was beneath the patch or involved the left atrial side of the septum.

Ablation was performed from the ASD patch to the superior vena cava for three tachycardias, from the high antero-septal to postero-septal aspect of the atrium for one tachycardia, between the ASD patch and the inferior vena cava for two tachycardias and between the ASD patch and

the tricuspid annulus for two tachycardias. Two patients had late recurrence of re-entry involving the ASD patch, with a different cycle length (Table 1). A repeat procedure abolished tachycardia in one of these two patients. Radiofrequency ablation successfully abolished IARTs in four of five patients.

Co-existence of multiple circuits. Eleven of 20 patients had circuits involving more than one of the three general areas described earlier. Four patients had circuits in all three areas. Different IARTs were recognized when IART terminated during RF ablation and subsequent programmed stimulation initiated a different IART using another circuit, or when IART shifted from one circuit to another during RF application or during entrainment.

Entrainment mapping at successful RF ablation sites. During IART, entrainment was generally performed before delivery of RF energy (Fig. 2 and 4). The PPI–TCL difference measured at 27 sites where RF terminated IART was ≤30 ms in all cases and averaged 4 ± 9 ms. However, RF failed to terminate IART at many sites when the PPI–TCL difference was <30 ms, consistent with ablation in a broad portion of the re-entry path. To assess whether a narrow isthmus could be detected from analysis of fusion during entrainment, we performed a retrospective analysis of the surface p wave morphology and intra-cardiac atrial activation sequence during entrainment from the 27 sites where RF terminated IART. In 10 cases (37%), p wave morphology could not be adequately assessed because the p waves were small and ill-defined or obscured by pacing artifact or a superimposed QRS complex. P wave morphology during entrainment could be compared with p wave morphology during tachycardia for 17 (63%) of 27 termination sites. At all 17 of these sites, entrainment occurred with concealed rather than manifest fusion (without an appreciable p wave change).

Electroanatomic mapping. In the initial group of patients in whom mapping was guided by fluoroscopy alone, RF ablation was successful in terminating 18 (86%) of 21 tachycardias and in rendering no tachycardias inducible in 4 (57%) of 7 patients. In the subsequent group of patients in whom entrainment mapping was combined with electroanatomic mapping, RF ablation was successful in terminating 20 (77%) of 26 tachycardias and in rendering no tachycardias inducible in 9 (69%) of 13 patients (p = NS). The mean fluoroscopic time per ablation session was 60 ± 30 min in patients with fluoroscopic guidance alone and 26 ± 9 min in patients in whom both fluoroscopic and electroanatomic guidance was used ($p < 0.001$).

Outcomes. Radiofrequency catheter ablation abolished 38 (81%) of 47 tachycardias in 18 (90%) of 20 patients. In 13 patients (65%), all 26 inducible tachycardias were abolished. In 5 patients (25%), 12 of 17 inducible tachycardias were abolished, but one tachycardia remained inducible. In two patients, ablation was completely unsuccessful; all four inducible tachycardias remained (the circuits appeared to involve the lateral right atrium in both patients). There were no complications of any of the procedures. Multiple procedures were performed in three of four patients (Patients 1, 2, 4 and 17) who had a recurrence after initially successful ablation. These revealed recurrence of a previously ablated circuit in one patient and previously undetected circuits in two patients. Repeat ablation abolished all inducible tachycardias in two of the three patients. Anti-arrhythmic therapy (amiodarone) was administered to 2 of 13 patients who had successful RF ablation of all IARTs. One of them had a history of atrial fibrillation, and the other patient developed paroxysmal atrial fibrillation 17 months after RF ablation. Anti-arrhythmic therapy was continued after ablation in three of five patients in whom RF ablation failed to suppress one of the inducible arrhythmias, and in one of the two patients in whom ablation failed to abolish any tachycardia (Table 1).

The mean follow-up period from the last ablation procedure was 19 ± 14 months (range 3 to 46). Overall, 12 of 13 patients who had successful ablation of all inducible macro–re-entrant circuits remained free of IART recurrence. Four of five patients who had one tachycardia inducible at the end of the procedure remained free of recurrence; three of them were treated with anti-arrhythmic drug therapy. Both patients who had unsuccessful ablation had recurrences. The cumulative risk of recurrence with RF ablation combined with anti-arrhythmic drug therapy (n = 6) was 20% at one and two years of follow-up.

DISCUSSION

Radiofrequency catheter ablation of IARTs in patients with previously repaired CHD is challenging for several reasons, as discussed in the present study and by other investigators (2,3,8). The anatomy is complex. Multiple circuits are frequent. The re-entry paths can be broad. In this study, we attempted to define the different types of re-entry circuits so that a systematic approach combining electroanatomic mapping and entrainment could be defined. In contrast to some studies (9), we attempted to ablate all inducible IARTs. Radiofrequency catheter ablation was successful in abolishing 38 (81%) of 47 inducible tachycardias.

We identified three general right atrial circuits: lateral wall circuits with re-entry around or related to the lateral atriotomy scar; septal circuits with re-entry around an ASD patch; and typical flutter circuits utilizing the isthmus between the tricuspid annulus and inferior vena cava. Left atrial macro–re-entrant circuits were infrequent in this group of patients. In a first set of patients, RF ablation was guided by entrainment mapping, and the problems encountered with this mapping approach were defined. In a second set of patients, three-dimensional electroanatomic mapping combined with entrainment mapping was used to address these problems and to guide RF ablation.

Entrainment mapping. Our initial mapping and ablative strategy was similar to that described by Triedman et al. (3)

and to that used for scar-related ventricular tachycardia (4). Entrainment mapping was used to determine if the Eustachian isthmus, lateral right atrium or atrial septum were in the re-entry circuit. When potential isthmuses were identified, entrainment adjacent to unexcitable areas that define the isthmus was used to determine whether they were, indeed, in the circuit. A line of RF lesions was applied to transect the isthmus.

Although entrainment mapping allowed localization of the substrate, supporting macro–re-entry and the design of an ablation strategy, there are several limitations. The PPI–TCL difference is short at sites in the re-entry circuit, regardless of whether the site is a narrow isthmus or a broad path. For example, in common atrial flutter, a relatively narrow isthmus is formed by the inferior vena cava and tricuspid annulus, where ablation is often effective. The lateral wall of the right atrium is a broad path in the circuit, which is difficult to transect with ablation. Once it is determined that the site is in the circuit, the degree of change in atrial activation (fusion) during entrainment is likely to be a better indicator of whether the region is a narrow isthmus, similar to observations in infarct-related ventricular tachycardia (4). However, fusion is difficult to assess on the surface ECG, because the pacing artifact and/or QRS complex often obscure the surface p waves, which often have a low amplitude in these patients. A retrospective analysis revealed that the degree of fusion could be determined for only 60% of the sites where RF was applied. Therefore, in addition to the PPI, anatomic information is useful to guide ablation, focusing on narrow circuit paths. When multiple potential re-entry circuits are present, pacing for entrainment can cause the rhythm to switch from one tachycardia circuit to another. If this change is not recognized, continued mapping produces confusing and conflicting information. Changes in the tachycardia from one circuit to another were also seen during application of RF current, presumably due to conduction block or slowing in one circuit, such that another becomes dominant. When this occurs, entrainment in the isthmus that is being transected indicates that it is a bystander potential. If division of that isthmus is abandoned prematurely, before the ablation line is completed, in favor of mapping the new tachycardia, the initial tachycardia may recur later. This problem complicated our initial procedures. We subsequently adopted the approach of attempting to complete a line of lesions across an isthmus, before beginning to map the next tachycardia.

Methodologic problems that can affect the validity of the PPI have been discussed previously (4). Decremental conduction during pacing increases the PPI, causing false negative assessment at some re-entry circuit sites. The potential presence of far-field potentials can also potentially impair the accuracy of entrainment mapping (Fig. 1). Finally, it is difficult to identify exact catheter positions in relation to anatomic barriers, because visualization of these barriers is not possible fluoroscopically. The difficulties created by some of these limitations can be reduced by combining entrainment mapping with electroanatomic mapping.

Three-dimensional electroanatomic mapping combined with entrainment mapping. An approach combining entrainment and electroanatomic mapping has been previously described for ablation of macro–re-entrant ventricular tachycardias. Nakagawa et al. (5) and Dorostkar et al. (6) described elegant examples of the use of three-dimensional electroanatomic mapping for ablation of IARTs after repair of complex CHD. We used this mapping system in association with entrainment mapping in 13 patients. The electroanatomic mapping system enables detailed mapping of the heart chambers, with accurate localization of anatomic barriers and zones of scar. Combining mapping of the activation sequence with entrainment mapping allows identification of the re-entry circuit, with fewer pacing attempts for entrainment. Broad paths are better defined, and individual RF lesions can be marked, facilitating transection of these paths. In addition, this approach allowed identification of a narrow isthmus where tachycardia was easily interrupted in three patients (Fig. 2 and 3). The location of an area of relatively focal spread from a region of scar was a marker of the exit from one of these narrow isthmuses. The presence of such an isthmus makes ablation of the circuit much easier than transecting a broad portion of the circuit with application of a long series of RF lesions. Circuits with a narrow isthmus were not identified in any of the initial seven patients in whom mapping was performed with entrainment alone. Although the success rate of RF ablation of IARTs was not different from that obtained with entrainment mapping alone, the fluoroscopy time was markedly shorter in the electroanatomic mapping group. This reduction was partly due to the fact that the catheter position could be continuously monitored during long, multiple RF applications without fluoroscopy. However, our understanding of the macro–re-entrant circuits responsible for IARTs also increased throughout the study period, likely contributing to shorter fluoroscopy times.

Acute effect of RF ablation and long-term outcome. Although our success rate is higher than those previously reported (2,3,8,9), direct comparisons are difficult, as studies differ not only in the ablation method, but also in the proportion of inducible IARTs targeted with ablation; the protocol used for programmed stimulation; the length of follow-up; the underlying disease and the nature of the remote surgical procedure; and the proportion of patients maintained on anti-arrhythmic therapy.

Conclusions. Ablation of macro–re-entrant atrial tachycardia late after repair of CHD is feasible and facilitated by a mapping approach that combines entrainment with activation mapping. In some cases, a narrow isthmus can be identified, where a relatively focal ablation is successful. In others, successful ablation can be achieved by a series of lesions across a broad path. Multiple re-entry circuits are common. Arrhythmia recurrences after an initially success-

ful ablation procedure often indicate the presence of other re-entry circuits in the scarred atrium.

Reprint requests and correspondence: Dr. William G. Stevenson, Cardiovascular Division, Brigham and Women's Hospital, 75 Francis Street, Boston, Massachusetts 02115. E-mail: wstevenson@rics.bwh.harvard.edu.

REFERENCES

1. Lesh MD, Kalman JM. To fumble flutter or tackle "tach"? Toward updated classifiers for atrial tachyarrhythmias. J Cardiovasc Electrophysiol 1996;7:460–6.
2. Kalman JM, Van Hare GF, Olgin JE, et al. Ablation of 'incisional' reentrant atrial tachycardia complicating surgery for congenital heart disease: use of entrainment to define a critical isthmus of conduction. Circulation 1996;93:502–12.
3. Triedman JK, Bergau DM, Saul JP, et al. Efficacy of radiofrequency ablation for control of intraatrial reentrant tachycardia in patients with congenital heart disease. J Am Coll Cardiol 1997;30:1032–8.
4. Stevenson WG, Khan H, Sager P, et al. Identification of reentry circuit sites during catheter mapping and radiofrequency ablation of ventricular tachycardia late after myocardial infarction. Circulation 1993;88:1647–70.
5. Nakagawa H, Jackman WM. Use of a three-dimensional, nonfluoroscopic mapping system for catheter ablation of typical atrial flutter. Pacing Clin Electrophysiol 1998;21:1279–86.
6. Dorostkar PC, Cheng J, Scheinman MM. Electroanatomical mapping and ablation of the substrate supporting intraatrial reentrant tachycardia after palliation for complex congenital heart disease. Pacing Clin Electrophysiol 1998;21:1810–9.
7. Shah DC, Jais P, Haissaguerre M, et al. Three-dimensional mapping of the common atrial flutter circuit in the right atrium. Circulation 1997;96:3904–12.
8. Van Hare GF, Lesh MD, Ross BA, et al. Mapping and radiofrequency ablation of intraatrial reentrant tachycardia after the Senning or Mustard procedure for transposition of the great arteries. Am J Cardiol 1996;77:985–91.
9. Baker BM, Lindsay BD, Bromberg BI, Frazier DW, Cain ME, Smith JM. Catheter ablation of clinical intraatrial reentrant tachycardias resulting from previous atrial surgery: localizing and transecting the critical isthmus. J Am Coll Cardiol 1996;28:411–7.